Regular Article

PHYSICAL CHEMISTRY RESEARCH
Published by the
Iranian Chemical Society
www.physchemres.org
info@physchemres.org

Phys. Chem. Res., Vol. 11, No. 4, 695-705, December 2023
DOI: 10.22036/pcr.2022.355336.2161

In Silico Study of the Effect of Porphyrin-Based Ligands on the Structure of G-Quadruplex in the Presence of Different Ions

F. Otovat[a], M.R. Bozorgmehr[b,*], A. Mahmoudi[a] and A. Morsali[b]

[a]*Faculty of Chemistry, Islamic Azad University, North Tehran Branch, Hakimiyeh, Tehran, Iran*

[b]*Department of Chemistry, Mashhad Branch, Islamic Azad University, Mashhad, Iran*

(Received 10 August 2022, Accepted 18 October 2022)

The interaction of planar porphyrins (L1), 5,10,15,20-tetrakis (1-ethyl-1-λ^4-pyridine-4-yl) porphyrin (L2), and 5,10,15,20-tetrakis (1-methyl-1-λ^4-pyridine-4-yl) porphyrin (L3) with G-quadruplex in the presence of Li^+, Na^+, K^+, Rb^+, Cs^+, Ca^{2+}, and Mg^{2+} ions was studied by density functional theory and molecular dynamics simulation. Single-point energy calculations were performed on sampled structures from molecular dynamics simulations. Sampling was performed by the free energy landscape (FEL). Quantum calculations were performed using the B3LYP density functional method with the 6-31G basis set. Quantum descriptors, frontier orbital energies, ionization energy, chemical hardness, chemical potential, and the number of transferred electrons were also calculated. The results showed that loops and sheets of G-quadruplex were involved in the interaction with ligands. The stability of the complex between ligands and G-quadruplex in the presence of K^+ and Na^+ ions was greater than that of the complex in the presence of Cs^+ and Mg^{2+} ions.

Keywords: Biosensor, Metal ion, Porphyrin, Quantum molecular descriptors, G-quadruplex

INTRODUCTION

Since guanines in DNA strands have a propensity to self-associate and bind to one another, the DNA structure in guanine-rich telomeric single-stranded regions can fold to form new intramolecular and intermolecular structures, known as G-quadruplex (GQ) [1-2]. In these structures, the four guanine bases come together due to sequence folding so that a quadruple planar arrangement, called G-quartet, is formed [1,3-4]. There are eight Hoogsteen hydrogen bonds on each quartet sheet. These bonds are formed by the bonding of N_1 and N_2 atoms of one guanine to N_7 and O_6 atoms of another guanine. Each guanine can be considered both a hydrogen-bond acceptor and donor [5-7]. The overlapping of two or more quartet sheets is caused by the π-π forces of GQ structures. GQ formation can play an important role in facilitating or preventing gene translation and or transcription [8-9]. In general, GQ can be divided into intramolecular groups (single molecule) and intermolecular groups (two and four molecules). The strands involved in GQ structures can have different orientations and produce parallel or non-parallel structures [10-13]. Molecular dynamics simulation studies show that the presence of cations in the quartet center contributes to the stability of the structure. The ions can be placed on the surface or between the quartet sheets, depending on the type and nature of the ion and the GQ structure [4,14-16]. Furthermore, the formation of GQ-ligand complexes can have a significant effect on the stability and efficiency of GQ. Some ligands facilitate the folding of strings as well as GQ formation and increase stability while others facilitate the unfolding of the structure and reduce stability [17-19]. Ligands can bind to GQ in different ways, including binding to the surface of G-quartet sheets *via* π-π stacking interactions or binding to loops or backbones (due to the charge transfer between the GQ and the ligand). Porphyrins, with large organic aromatic rings, are considered to be important ligands in the GQ-ligand complex due to their structural properties and wide applications, especially in

*Corresponding author. E-mail: bozorgmehr@mshdiau.ac.ir

modern drug delivery systems [20-21]. Hemin and vitamin B12 are among the most prominent of these structures that express the special status of GQ complexes in living environments. Studies on GQ complexes with porphyrin derivatives indicate that these ligands can enhance the stability of the structures and be used to inform a wide range of applications for these complexes [22-23]. For example, these complexes can be used as biosensor probes due to their ability to bind to metal ions and other analytes [24-25]. DNAzyme and aptameters are examples of such applications, in which detection is based on non-covalent interactions of the structure with the target molecule. These interactions include hydrogen bonds, π-π stacking interactions, Van der Waals, and electrostatic and hydrophobic interactions. For example, biosensors are used to detect heavy ions. Increasing some of these ions in vital human organs can lead to nucleotide acid dysfunction, immune deficiencies, nervous system dysfunction, anemia, cardiovascular diseases, decreased intelligence and learning ability, developmental damage, and even death. For this reason, many health organizations worldwide have examined the safety limits of these ions in medicine, food, and drinking water. Therefore, the development of a simple and rapid method with high affinity and specificity is essential to simultaneously monitor the concentration of metal ions and other analytes. In this regard, DNAzymed-based biosensors and aptasensors are the two major groups of functional nucleic acids (FNA) that have received much attention [26-28].

Theoretical approaches can provide useful information about the type and quality of the interactions of the above-mentioned structures that are time-consuming and expensive to study and are not observable on a laboratory scale. It is not possible to investigate the sensory properties and electrochemical activity of compounds using molecular dynamics simulations. In such cases, quantum computing can provide a great deal of information. In this study, the interactions of porphyrin ligands, 5,10,15,20-tetrakis (1-ethyl-1-λ4-pyridine-4-yl) porphyrin, and 5,10,15,20-tetrakis (1-methyl-1λ4-pyridine-4-yl) porphyrin with GQ were determined using molecular dynamics simulations. Quantum calculations of the GQ structure in the presence of Mg^{2+}, Cs^{+}, Rb^{+}, K^{+}, Na^{+}, Li^{+}, and Ca^{2+} were also carried out to investigate the reactivity and stability of the complexes.

METHODS

The GQ structure with the entry 1KF1 was obtained from the protein databank [29]. Its sensor property is related to the sheet-like structure of its guanines. At least, three factors have been found to play a role in the stability of GQ sheets: intra-quartet hydrogen bonds, inter-quartet stacking, and cation coordination. Therefore, it is important to study the role of cations in the stability of GQ. For this purpose, lithium, sodium, potassium, cesium, rubidium, magnesium, and calcium ions were placed in the center of three quartets of the GQ structure using the software PyMol [30]. Table 1 presents the basis of the designed simulation boxes.

In all designed simulation boxes, the GQ was placed in the center of the box, and ligands were randomly placed in the boxes. All boxes were filled with the TIP3P water model. In the quadruplex structure, there were negatively charged phosphate groups. In addition, three cations were placed in the center of the quadruplex sheets. Therefore, the total system charge was negative. Thus, an appropriate number of sodium ions was added to each box to neutralize the whole system. Molecular dynamics simulation calculations were performed using Gromacs version 5.1.2 and the AMBER force field ff99SB [31]. Since Gromacs does not have the force field parameters of the ligands by default, these parameters were obtained from the AmberTools package [32]. For this purpose, the ligand structure was optimized using the density functional theory (DFT) method with the basis set of 6-31G by the GAMESS software [33]. To control the optimization of structures, frequency calculations were

Table 1. The Designed Systems (S_0, S_1, S_2, S_3)

System	GQ	ION	L1	L2	L3
S_0	+	+	-	-	-
S_1	+	+	+	-	-
S_2	+	+	-	+	-
S_3	+	+	-	-	+

Ion: Li^{+}, Na^{+}, K^{+}, Rb^{+}, Cs^{+}, Ca^{2+}, Mg^{2+}. L1: Porphyrin. L2: 5,10,15,20-tetrakis (1-ethyl-1 λ4-pyridin-4-yl) porphyrin. L3: 5,10,15,20-tetrakis(1-methyl-1λ4-pyridin-4-yl) porphyrin.

carried out at the same level using the DFT method and no virtual frequency was observed. To eliminate the frictional contacts between particles in the simulation boxes, all systems were minimized in terms of energy using the steepest descent method. In two steps, the systems were equilibrated in NVT and NPT ensembles, each for 5 nanoseconds at the time step of 2 fs, respectively. In the final step, the molecular dynamics simulation was performed for 500 nanoseconds at a time step of 2 fs. To increase the accuracy of the simulations and to avoid the dependency of results on initial conditions, each simulation was repeated three times under different initial conditions. The system temperature and pressure were controlled in all simulation runs using V-rescale and Berendsen thermostats, respectively [34-35]. The chemical bond between GQ and the ligands was constrained using the LINCS algorithm, and the chemical bonds of water molecules were constrained using the SETTLE algorithm [36]. The PME algorithm was used to calculate electrostatic interactions [37]. Enhanced sampling has always been at the core of molecular dynamics simulations. The last few nanoseconds of simulation or those of the equilibrium condition are averaged and sampled to enhance the quality of sampling [38-39]. In these methods, although variations in the quantity, such as Cα-RMSD in the core region, are used, there is no physical concept in the average of atomic coordinates [40]. Thus, simulations were sampled by the FEL [41]. The FEL included the following three main stages: Calculating the root-mean-square deviation (RMSD) and the radius of gyration (Rg), examining the possibility of the presence of protein configuration in corresponding values of RMSD and Rg, and calculating the free energy of protein configurations based on their presence probability values. The results of the FEL analysis are shown in 3D diagrams in Fig. 1. In these diagrams, areas with minimum free energy are shown in blue. Diagrams show that there was a local minimum free energy in all cases, suggesting that the GQ had a stable configuration in the presence of ligands.

Ab initio analysis was performed on sampling structures obtained from molecular dynamics simulations. Moreover, single-point energy calculation was performed on sampled structures. The DFT method with previous specifications was used for these calculations.

RESULTS AND DISCUSSION

GQ structures were found to react with ligands in different ways to form GQ-ligand complexes. Porphyrins, whose core had a structure similar to that of G-quartet sheets in GQ (Fig. 2), bound to GQ through the loops and the surface of quartet sheets.

The stability and reactivity of the systems presented in Table 2 were investigated using quantum descriptors. Factors such as the energy of the highest occupied molecular orbital (EHOMO), the energy of the lowest unoccupied molecular orbital (ELUMO), and the energy difference between the two orbitals (E_{gap}) are among the most important parameters used in quantum investigations [42]. E_{gap} is typically considered as the distance between the α-HOMO and β-LUMO orbitals.

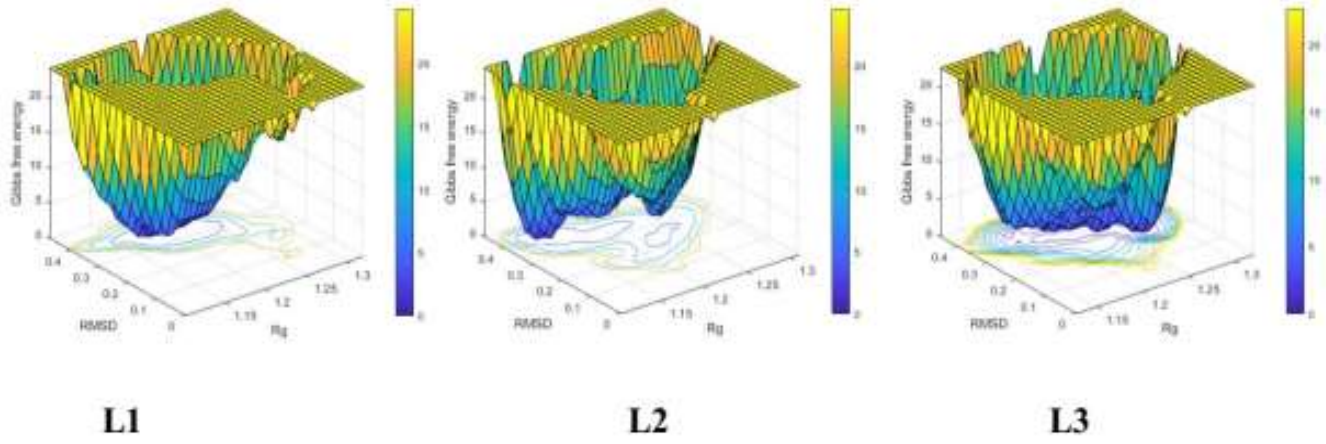

Fig. 1. The FLE of the simulated systems in the presence of L1, L2, L3, and K^+ ions.

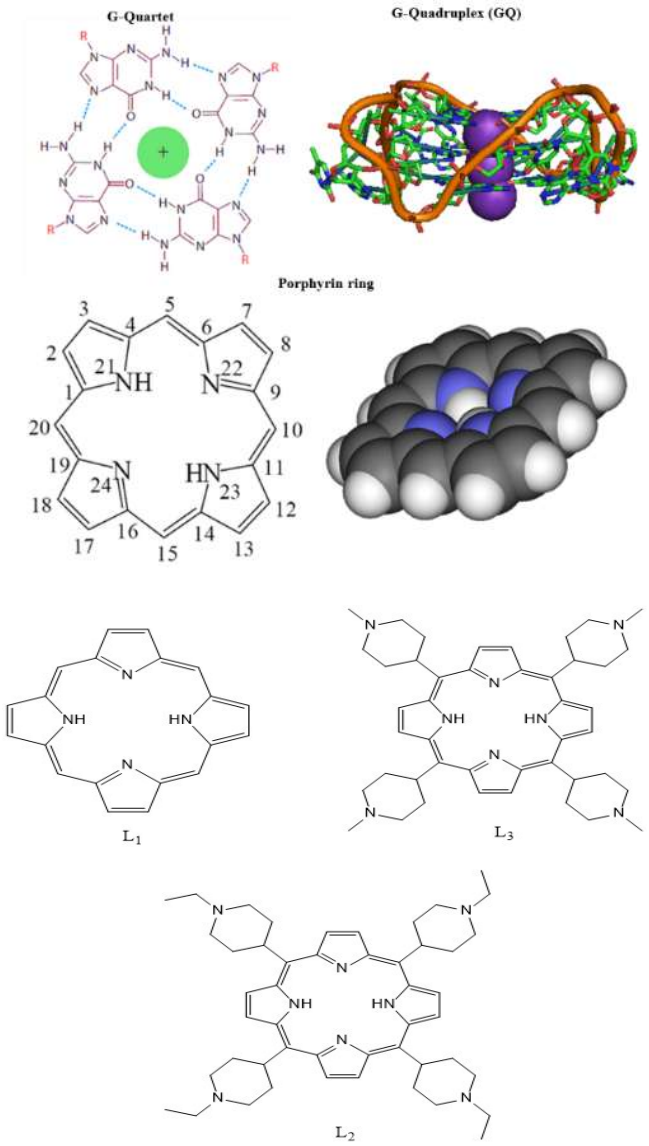

Fig. 2. A comparison of GQ (1KF1) and porphyrin ring structures along with the chemical structures of studied ligands.

If both electron orbitals with the spin α or β are identical in terms of density distribution, both can be considered as the descriptors of these electron orbitals. Therefore, in this study, the gap between α-HOMO and α-LUMO, which is physically significant, was considered as the criterion for calculating E_{gap} [43].

Compounds that have high E_{gap} require more energy to transmit electrons to the excited state, resulting in greater stability. In addition, it has been established that there is a good linear correlation between the calculated E_{HOMO} and the ionization energy (I), between E_{LUMO} and electron affinity (A), and between E_{gap} and chemical hardness (η), chemical potential (μ), and the number of transferred electrons (ΔN). The above-mentioned measurement indices were calculated from Eqs. (1) to (6) using E_{HOMO} and E_{LUMO} [42], and the results are listed in Tables 2 and 3.

$$I = -E_{HOMO} \quad (1)$$

$$A = E_{LUMO} \quad (2)$$

$$E_{gap} = E_{Lumo} - E_{HOMO} \quad (3)$$

$$H = \frac{(I-A)}{2} \quad (4)$$

$$\mu = \frac{-(I+A)}{2} \quad (5)$$

$$\Delta N = \mu_{GQ} - \frac{\mu_{ligand}}{2(\eta_{ligand}-\eta_{GQ})} \quad (6)$$

According to Table 2, among the ligands, L_2 had the lowest E_{gap} in most cases (except in the presence of Rb^+ and Cs^+) and L_1 had the highest E_{gap} in all cases. Since any decrease in E_{gap} is associated with a decrease in stability, L_2 was expected to be more unstable than the other species and easier to react with GQ. In all four modes considered for GQ, the calculated values for E_{gap} did not differ significantly, and only GQ_{S0} showed a slight difference in the presence of Li^+ and K^+ ions. Electron affinity analysis showed that the values of A for ligands were as follows: $L_3 < L_2 < L_1$. The highest and lowest values of A among the ligands were -729.14 and -561.93 kJ mol^{-1}, which were related to the S_1 system in the presence of Mg^{2+} and to the S_3 system in the presence of K^+, respectively. The difference between electron affinities for different GQ systems was very small.

The examination of the ionization energy (I) showed that the values obtained from L_2 and L_3 were significantly different from those of the other species and were the lowest among the species studied ($L_3 < L_2 <$ other species). L_1 had more ionization energy than the other ligands, indicating that these values were very close to those obtained from GQs. The values of global hardness (η), which is a measure of the

Table 2. Calculated Quantum Molecular Descriptors (kJ mol^{-1}) for the Optimized Systems

Ion	Species	E_{HOMO}	E_{LUMO}	E_{gap}	η	μ
	GQ_{s0}	-763.02	-425.40	377.62	168.81	-594.21
	GQ_{S1}	-772.30	-429.22	343.07	171.54	-600.76
	GQ_{S2}	-766.13	-426.50	339.63	169.81	-599.46
Li^+	GQ_{S3}	-771.44	-427.49	343.95	171.97	-594.34
	$Ligand_{S1}$	-771.07	-719.39	51.67	25.84	-745.23
	$Ligand_{S2}$	-684.12	-673.19	10.93	5.46	-678.65
	$Ligand_{S3}$	-578.33	-564.24	14.08	7.04	-572.99
	GQ_{s0}	-769.64	-428.86	340.78	170.39	-599.25
	GQ_{S1}	-765.08	-434.57	330.51	165.25	-599.82
	GQ_{S2}	-764.16	-423.43	340.73	170.36	-593.78
Na^+	GQ_{S3}	-765.22	-425.79	339.43	169.71	-595.50
	$Ligand_{S1}$	-765.76	-720.42	45.33	22.67	-743.09
	$Ligand_{S2}$	-686.71	-673.86	12.85	6.42	-680.29
	$Ligand_{S3}$	-593.18	-575.00	18.18	4.41	-581.15
	GQ_{s0}	-767.18	-428.43	388.74	169.37	-597.80
	GQ_{S1}	-769.08	-429.89	339.19	169.60	-599.49
	GQ_{S2}	-764.78	-422.10	342.68	171.34	-599.61
K^+	GQ_{S3}	-767.17	-432.54	334.14	167.07	-599.98
	$Ligsnd_{S1}$	-764.51	-722.48	42.03	21.01	-738.77
	$Ligand_{S2}$	-681.58	-672.39	9.19	4.59	-672.39
	$Ligand_{S3}$	-600.57	-561.93	38.63	19.32	-581.25
	GQ_{s0}	-767.77	-425.60	342.18	170.96	-596.68
	GQ_{S1}	-768.45	-430.85	337.60	168.80	-599.65
	GQ_{S2}	-772.58	-428.34	344.24	174.48	-600.46
Rb^+	GQ_{S3}	-757.53	-431.16	326.36	163.18	-594.34
	$Ligand_{S1}$	-764.62	-721.43	43.19	21.60	-743.03
	$Ligand_{S2}$	-688.75	-680.90	7.85	3.92	-684.82
	$Ligand_{S3}$	-595.47	-588.33	7.13	3.57	-591.90
	GQ_{s0}	-769.21	-427.82	341.38	170.69	-598.52
	GQ_{S1}	-766.73	-428.73	337.98	168.99	-597.74
	GQ_{S2}	-770.58	-425.68	344.89	172.44	-599.46
Cs^+	GQ_{S3}	-772.75	-427.22	345.53	172.76	-599.98
	$Ligand_{S1}$	-765.58	-718.76	46.82	23.41	-742.17
	$Ligand_{S2}$	-690.62	-667.72	22.90	11.45	-679.05
	$Ligand_{S3}$	-591.03	-582.86	8.17	4..08	-586.95
	GQ_{s0}	-761.37	-427.99	333.37	166.69	-594.68
	GQ_{S1}	-767.01	-434.62	332.38	166.19	-600.81
	GQ_{S2}	-765.81	-425.88	339.93	169.96	-597.09
Ca^{2+}	GQ_{S3}	-771.27	-422.91	348.36	174.18	-597.09
	$Ligand_{S1}$	-756.77	-716.93	39.84	19.92	-736.85
	$Ligand_{S2}$	-692.77	-680.66	11.32	5.66	-687.11
	$Ligand_{S3}$	-594.07	-580.35	13.72	6.86	-587.21
	GQ_{s0}	-766.21	-426.56	339.65	169.82	-596.38
	GQ_{S1}	-773.42	-434.40	339.02	169.51	-603.91
	GQ_{S2}	-769.46	-427.92	341.54	170.76	-598.69
Mg^{2+}	GQ_{S3}	-767.00	-428.56	338.45	169.22	-597.78
	$Ligand_{S1}$	-773.07	-729.14	43.93	21.96	-751.11
	$Ligand_{S2}$	-688.69	-680.84	3.79	1.90	-686.73
	$Ligand_{S3}$	-585.55	-576.75	8.80	9.09	-584.09

resistance of a chemical species to changes in its electronic structure, were generally higher for GQ than the ligands, indicating that the ligands were generally softer than GQs, had higher reactivity and lower stability, and could more easily enter into chemical reactions. Among GQs, the highest and the lowest η values (174.48 kJ mol^{-1} and 163.18 kJ mol^{-1}, respectively) in the presence of Rb^+ were found in GQ_{S2} and GQ_{S3}. Among the ligands, L_1 had higher η values than the other two ligands. The highest and lowest η values among the ligands were 25.84 and 1.90 kJ mol^{-1}, which corresponded to L_1 in the presence of Li^+ ion and L_2 in the presence of Mg^{2+} ion, respectively.

The chemical potential (μ), which is one of the most important parameters in evaluating the reactivity of systems, was studied to investigate the tendency of electrons to leave the equilibrium. The two ligands L_1 and L_2 had the highest μ values among all species, respectively. The lowest and the highest μ values for L_1 were found to be -736.85 kJ mol^{-1} (for Ca^{2+}) and -751.11 kJ mol^{-1} (for Mg^{2+}), respectively. Moreover, -672.39 kJ mol^{-1} was the lowest and -687.11 and -686.73 kJ mol^{-1} were the highest μ values for L_2 and were related to K^+, Ca^{2+}, and Mg^{2+}, respectively. The μ values obtained for L_3 and GQs were approximately the same.

The ΔN index, which describes the charge transfer, was calculated from Eq. (6) for systems S_1, S_2, and S_3, and the results are listed in Table 3.

The ΔN values obtained for the above three systems were negative, revealing that the direction of the charge current in them was from ligand to GQ. Therefore, GQ was considered as the electron acceptor and the ligands as the electron donor in all the systems. In general, S_3 and S_1 had the lowest and highest value of ΔN (transferred electron), respectively. Since in the GQ structure, the four G-quartet sheets were overlapped by π-π staking forces at a certain distance, the study of these forces provided useful information about the GQ structure and its variation in different conditions and environments. The distance between the corresponding guanines on the adjacent G-quartet sheets was measured in all systems, and the results are presented in Table 4. Also, the distance of the 1KF1 sequence sheets, the file of which was extracted from the PDB database, was measured as a reference, as shown in Fig. 3. Any deviation from these values, which together were considered to be the standard state, was considered to indicate a change in the stability of the GQ structure in the presence of various ions and ligands. According to the values obtained from Table 4, the structure of GQ in S_0 changed less in the presence of K^+ and Na^+ ions than in the presence of other ions. The maximum deviation from the ground state (1KF1) occurred due to the presence of Mg^{2+} ion. The images obtained from molecular dynamics simulation showed that the guanines involved in the formation of sheets were displaced. The distance between the 3-3 guanines of the first and the second sheets and the 4-4 guanines between the second and third sheets (d_{Down}) was greater than 6 Å (6.41 and 6.03, respectively). The upper 3-3 guanines in the presence of lithium ions had a distance of 3.36 Å from each other, which was far from the base state.

Table 3. The Calculated Partial Number of Electrons Transferred from Ligands to GQ in 3 Systems

Ion	ΔN		
	S1	S2	S3
Li^+	-2.79	-2.29	-1.94
Na^+	-2.83	-2.30	-1.98
K^+	-2.71	-2.24	-2.19
Rb^+	-2.77	-2.24	-2.08
Cs^+	-2.78	-2.34	-1.97
Mg^{2+}	-2.77	-2.26	-2.05
Ca^{2+}	-2.75	-2.28	-1.98

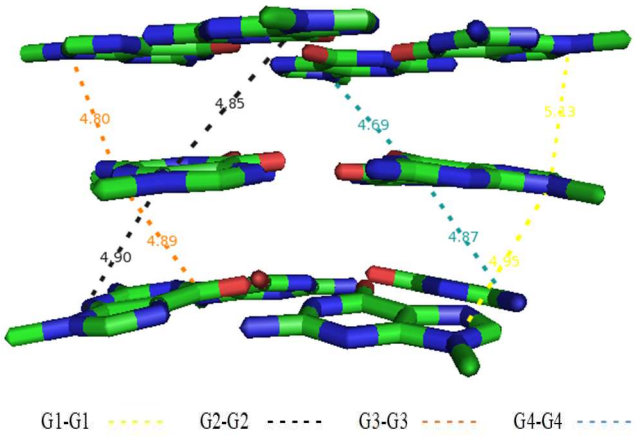

Fig. 3. The calculated distance between the corresponding guanines of 1KF1.

Table 4. The Calculated Distance between Corresponding Guanines in Different Systems

System		S_0		S_1		S_2		S_3	
ION	Guanine number	d_{Up}	d_{Down}	d_{Up}	d_{Down}	d_{Up}	d_{Down}	d_{Up}	d_{Down}
Li^+	1-1	4.98	4.79	4.77	5.29	3.59	5.21	4.16	4.81
	2-2	4.53	5.24	3.88	4.06	5.23	4.50	5.04	4.54
	3-3	3.36	4.55	3.85	5.23	5.73	5.00	3.84	5.18
	4-4	4.61	4.48	4.08	4.93	4.28	4.55	3.73	5.29
Na^+	1-1	4.81	4.74	4.75	4.27	3.99	4.94	3.84	5.30
	2-2	4.99	4.59	4.52	4.69	4.46	5.61	4.23	4.72
	3-3	5.13	4.78	5.13	5.09	4.13	4.64	3.67	4.58
	4-4	5.19	4.74	4.73	5.21	4.24	5.10	4.06	4.88
K^+	1-1	5.51	4.98	4.48	4.64	4.73	4.43	4.12	4.92
	2-2	4.76	4.49	5.25	4.94	5.26	4.89	3.62	5.05
	3-3	4.71	4.66	4.46	5.09	4.40	4.60	4.07	4.68
	4-4	4.43	4.82	4.70	4.53	5.13	5.08	3.75	5.44
Rb^+	1-1	4.52	4.53	4.25	4.90	4.86	4.70	4.73	5.19
	2-2	4.53	5.05	4.54	4.63	4.66	4.83	4.04	5.61
	3-3	4.44	5.02	4.15	4.53	4.84	4.21	4.19	4.70
	4-4	5.07	5.10	3.93	4.92	5.23	4.85	5.52	4.79
Cs^+	1-1	3.81	5.01	6.43	4.27	3.96	4.85	4.74	4.54
	2-2	3.87	4.88	3.63	4.76	4.31	4.80	4.79	4.49
	3-3	4.39	5.25	4.69	4.33	3.72	5.52	4.98	4.83
	4-4	4.84	4.41	3.87	4.96	4.09	5.08	4.27	3.67
Mg^{2+}	1-1	5.43	4.37	5.78	4.79	5.12	5.14	7.23	4.32
	2-2	5.18	5.47	5.31	6.31	5.03	4.95	5.35	4.84
	3-3	6.41	4.37	3.97	4.66	5.09	4.93	5.39	5.05
	4-4	4.78	6.03	6.44	4.66	9.82	4.20	6.34	4.01
Ca^{2+}	1-1	4.30	4.43	4.75	4.58	5.19	4.82	5.23	4.73
	2-2	4.74	4.55	4.68	4.86	5.43	4.47	3.71	5.01
	3-3	4.11	4.67	4.55	4.69	5.05	4.70	4.58	5.09
	4-4	4.58	5.11	5.02	4.41	4.67	4.71	5.09	5.04

While the sheets were slightly displaced in the presence of lithium ions, they did not show a noticeable change in the presence of other ions despite displacements relative to 1KF1. In system S1, it was observed that the changes in the

presence of the ligand were greater than those in the absence of the ligand. In this system, the K^+ and Na^+ ions had the nearest values to 1KF1, and the shapes of the sheets were well preserved. In the presence of Ca^{2+} and Rb^+ ions, with slight changes in the structure and distance between the sheets, the G-quartet guanine order was almost unchanged. However, values less than 4 Å and more than 5 Å were observed for other ions and the deviation from the ground state was higher for these ions than the reference ions.

The GQ structure in system S1, containing Cs^+ and Mg^{2+}, was completely changed. In system S_2, except for the ion Mg^{2+}, where the upper sheet guanine was completely dissociated and had a distance of 9.82 Å from the second sheet guanine, the other ions do not cause a significant change in the structure of G-quartet sheets despite the changes between the sheets relative to 1KF1. In general, despite the variations in the intersheet spacing in this system, the GQ structure in the presence of all ions was better preserved than in other systems and the sheets were in better order.

In system S_3, the measured values were quite different from 1KF1 in the presence of Mg^{2+} ion and the GQ structure was lost. In the presence of Cs^+ ion, however, the deviation in the space between the sheets was not significant relative to 1KF1 and the GQ structure was completely changed (Fig. 4).

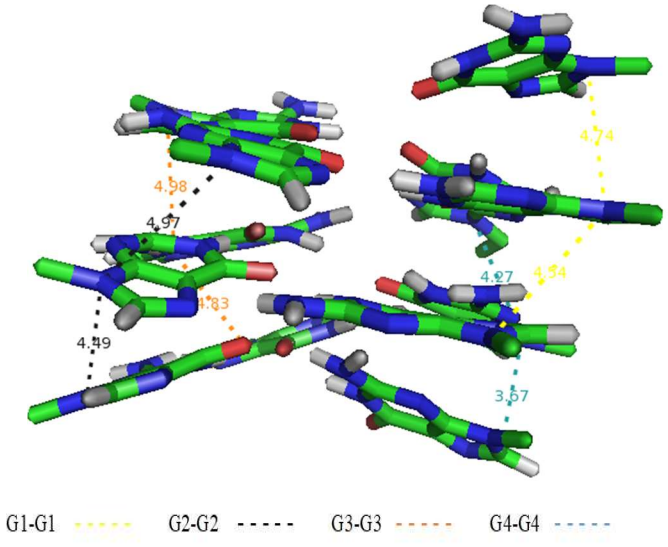

Fig. 4. The calculated distance between the corresponding guanines of 1KF1 in the presence of Cs^+ ion.

As regards the other ions, the GQ structure did not undergo any significant changes and the sheets were regular and close to the ground state.

CONCLUSIONS

To investigate the structural and sensory properties of GQ-ligand complexes, π-π stacking interactions, energy changes, electronic changes of the GQ structure, and three porphyrin-based ligands were studied by quantum computing in three systems, namely, S_0, S_1, S_2, and S_3, and in the presence of different ions. The ligand and ions caused changes in the structure of GQ relative to the ground state. An examination of the π-π forces showed that L_2 and L_3 complexes retained the GQ structure more stable than did the GQ-L_1 complex despite the variation in the space between the quartet sheets. Energy calculations showed that L_1 (a porphyrin-based ligand consisting of only a non-substituted ring) was generally less inclined to interact with GQ whereas the other two ligands, with a substitution on the porphyrin ring, interacted more easily with GQ. Experimental studies on GQ and porphyrin derivatives have also shown that the substituent on the porphyrin ring facilitates loops and sheets attachment as well as GQ-ligand binding. For example, a study of two ligands, called TMPyP4 and TPrPyP4, showed that TPrPyP4, with a larger substituent, had generally stronger interactions with GQ [23,44-46]. The ionization energy analysis also showed that the calculated energy of L_1 was similar to that of GQ, which could be due to the structural similarity of L_1 to the G-tetrad plane. The ΔN values, indicating the rate of charge transfer between the species involved, showed that the direction of the electron current in the studied systems was from the ligand to GQ. In this study, the highest charge transfer was observed in system S_1. The electronic and structural changes in the biological environment are the basis of biosensors, in which the detection is made by measuring an identifiable change or signal. Given that the performance evaluation of a biochemical sensor depends on the interactions at the molecular level, the information obtained in this study can be useful in designing and manufacturing biosensors with high selectivity and specificity for use in specific biological applications.

REFERENCES

[1] Burge, S.; Parkinson, G. N.; Hazel, P.; Todd, A. K.; Neidle, S., *Nucleic Acids Res.*, **2006,** *34*, 5402-5415, DOI: 10.1093/nar/gkl655.

[2] Kolesnikova, S.; Curtis, E. A., Structure and Function of Multimeric G-quadruplexes. *Molecules*, **2019**, *24* (17), 3074-3094, DOI: 10.3390/molecules24173074.

[3] Day, H. A.; Pavlou, P.; Waller, Z. A., i-Motif DNA: structure, stability and targeting with ligands. *Bioorg. Med. Chem*., **2014**, *22* (16), 4407-4418, DOI: 10.1016/j.bmc.2014.05.047.

[4] Davis, J. T., G-quartets 40 years later: from 5′-GMP to molecular biology and supramolecular chemistry. *Angew Chem. Int. Ed. Engl*., **2004**, *43* (6), 668-698, DOI: 10.1002/anie.200300589.

[5] Ghoshdastidar, D.; Bansal, M., Dynamics of physiologically relevant noncanonical DNA structures: an overview from experimental and theoretical studies. *Brief. Funct. Genomics*, **2018**, *18*, 192-204, DOI: 10.1093/bfgp/ely026.

[6] Williamson, J. R.; G-quartet structures in telomeric DNA. *Annu. Rev. Biophys.*, **1994**, *23* (1), 703-730, DOI: 10.1146/annurev.bb.23.060194.003415.

[7] Zimmerman, S. B.; Cohen, G. H.; Davies, D. R., X-ray fiber diffraction and model-building study of polyguanylic acid and polyinosinic acid. BBA Adv., **1975**, *92* (2), 181-192, DOI: 10.1016/0022-2836(75)90222-3.

[8] Bhattacharyya, D.; Mirihana Arachchilage, G.; Basu, S., Metal cations in G-quadruplex folding and stability. *Front Chem*., **2016**, *4,* 38-52, DOI: 10.3389/fchem.2016.00038.

[9] Yakovchuk, P.; Protozanova, E.; Frank-Kamenetskii, M. D., Base-stacking and base-pairing contributions into thermal stability of the DNA double helix. *Nucleic Acids Res.*, **2006**, *34* (2), 564-574, DOI: 10.1093/nar/gkj454.

[10] Bochman, M. L., Paeschke, K.; Zakian, V. A., DNA secondary structures: stability and function of G-quadruplex structures. *Nat. Rev. Genet*, **2012**, *13* (11), 770-780, DOI: 10.1038/nrg3296.

[11] Keniry, M. A., Quadruplex structures in nucleic acids. *Biopolymers: Original. Res. Biomol*., **2000**, *56* (3), 123-146, DOI: 10.1002/1097-0282(2000/2001)56:3<123::AID-BIP10010>3.0.CO;2-3.

[12] Esposito, V., *et al*., A topological classification of G-quadruplex structures. Nucleosides, Nucleotides *Nucleic Acids*, **2007**, *26* (8-9), 1155-1159, DOI: 10.1080/15257770701527059.

[13] Nasiri, A. H., *et al*., An intermolecular G-quadruplex as the basis for GTP recognition in the class V-GTP aptamer. *RNA*, **2016**, *22* (11), 1750-1759, DOI: 10. 2211/1750.short.

[14] Basu, S., *et al*., Direct detection of monovalent metal ion binding to a DNA G-quartet by 205Tl NMR. *JACS*, **2000**, *122* (13), 3240-3241, DOI: 10.1021/ja993614g.

[15] Cai, M., *et al*., Cation-directed self-assembly of lipophilic nucleosides: the cation's central role in the structure and dynamics of a hydrogen-bonded assembly. *Tetrahedron*, **2002**, *58* (4), 661-671, DOI: 10.1016/S0040-4020(01)01101-2.

[16] Miyoshi, D., *et al*., Effect of divalent cations on antiparallel G-quartet structure of d (G4T4G4). *FEBS letters*, **2001**, *496* (2-3), 128-133, DOI: 10.1016/S0014-5793(01)02416-4.

[17] Haider, S. M.; Neidle, S.; Parkinson, G. N., A structural analysis of G-quadruplex/ligand interactions. *Biochimie*, **2011**, *93* (8), 1239-1251, DOI: 10.1016/j.biochi.2011.05.012.

[18] Murat, P.; Singh, Y.; Defrancq, E., Methods for investigating G-quadruplex DNA/ligand interactions. *Chem. Soc. Rev*., **2011**, *40* (11), 5293-5307, DOI: 10.1039/C1CS15117G.

[19] Uda, R. M.; Matsui, T.; Takei, M., Binding of malachite green promotes stability and shows preference for a human telomere DNA G-quadruplex. *Supramolecular Chem.*, **2017**, *29* (8), 553-560.

[20] Wei, C., *et al*., Study on the interaction of porphyrin with G-quadruplex DNAs. *Biophy. Chem*., **2008**, *137* (1), 19-23, DOI: 10.1080/10610278.2017.1297447.

[21] Hou, J. -Q., *et al*., New insights into the structures of ligand-quadruplex complexes from molecular dynamics simulations. *J. Phys. Chem. B*, **2010**, *114* (46), 15301-15310, DOI: 10.1021/jp106683n.

[22] Izbicka, E., *et al*., Effects of cationic porphyrins as G-quadruplex interactive agents in human tumor cells.

Cancer Res., **1999**, *59* (3), 639-644, DOI: 10. 2231/1648.cr.

[23] Wei, C., *et al*., A spectroscopic study on the interactions of porphyrin with G-quadruplex DNAs. *Biochem*., **2006**, *45* (21), 6681-6691, DOI: 10.1021/bi052356z.

[24] Han, H., *et al*., Selective interactions of cationic porphyrins with G-quadruplex structures. *JACS*, **2001**, *123* (37), 8902-8913, DOI: 10.1021/ja002179j.

[25] Ruttkay-Nedecky, B., *et al*., G-quadruplexes as sensing probes. *Molecules*, **2013**, *18* (12), 14760-14779, DOI: 10.3390/molecules181214760.

[26] McKeague, M.; DeRosa, M. C., Challenges and opportunities for small molecule aptamer development. *J. Nucleic Acids*, **2012**, *2012*, 1-21, DOI: 10.1155/2012/748913.

[27] Khoshbin, Z., *et al*., Simultaneous detection and determination of mercury(II) and lead(II) ions through the achievement of novel functional nucleic acid-based biosensors. *Biosens. Bioelectron*., **2018**, *116*, 130-147, DOI: 10.1016/j.bios.2018.05.051.

[28] Housaindokht, M. R.; Verdian-Doghaei, A., Biophysical probing of the binding properties of a Cu(II) complex with G-quadruplex DNA: an experimental and computational study. *Luminescence*, **2016**, *31* (1), 22-29, DOI: 10.1002/bio.2916.

[29] Parkinson, G. N.; Lee, M. P.; Neidle, S., Crystal structure of parallel quadruplexes from human telomeric DNA. *Nature*, **2002**, *417* (6891), 876-880, DOI: 10.1038/nature755.

[30] DeLano, W. L., Pymol: An open-source molecular graphics tool. CCP4 News. *Prot. Crystal*, **2002**, *40* (1), 82-92, DOI: 10. 2041/1866.py.

[31] Lindorff-Larsen, K., *et al*., Improved side-chain torsion potentials for the Amber ff99SB protein force field. *Proteins: Struct. Func. Bioinformatics*, **2010**, *78* (8), 1950-1958, DOI: 10.1002/prot.22711.

[32] Macke, T. J., *et al*., AmberTools Users' Manual. **2010**,

[33] Gordon, M. S.; Schmidt, M. W., Advances in electronic structure theory: GAMESS a decade later, in Theory and applications of computational chemistry. **2005**, 1167-1189, DOI: 10.1016/B978-044451719-7/50084-6.

[34] Bussi, G.; Donadio, D.; Parrinello, M., Canonical sampling through velocity rescaling. *J. Chem. Phys.*, **2007**, *126* (1), 014101, DOI: 10.1063/1.2408420.

[35] Berendsen, H. J., *et al*., Molecular dynamics with coupling to an external bath. *J. Chem. Phys*., **1984**, *81* (8), 3684-3690, DOI: 10.1063/1.448118.

[36] Hess, B., *et al*., LINCS: a linear constraint solver for molecular simulations. *J. Comp. Chem*., **1997**, *18* (12), 1463-1472, DOI: 10.1002/(SICI)1096-987X(199709)18:12<1463::AID-JCC4>3.0.CO;2-H.

[37] Darden, T.; York, D.; Pedersen, L., Particle mesh Ewald: An N· log(N) method for Ewald sums in large systems. *J. Chem. Phys*., **1993**, *98* (12), 10089-10092, DOI: 10.1063/1.464397.

[38] Housaindokht, M. R., *et al*., Structural properties of the truncated and wild types of Taka-amylase: A molecular dynamics simulation and docking study. *J. Mol. Cat. B: Enzym*., **2013**, *95*, 36-40, DOI: 10.1016/ j.molcatb.2013.05.011.

[39] Moghtaderi, N.; Bozorgmehr, M. R.; Morsali, A., The study of self-aggregation behavior of the bilirubin molecules in the presence and absence of carbon nanotubes: Molecular dynamics simulation approach. *J. Mol. Liq*., **2015**, *208*, 342-346, DOI: 10.1016/ j.molliq.2015.04.052.

[40] van der Spoel, D., *et al*., GROMACS user manual version 3.3. **2008**.

[41] Lei, H., *et al*., Folding free-energy landscape of villin headpiece subdomain from molecular dynamics simulations. *Proc. Nat. Acad. Sci*., **2007**, *104* (12), 4925-4930, DOI: 10.1073/pnas.0608432104.

[42] Mansoorinasab, A., *et al*., Quantum mechanical study of carbon nanotubes functionalized with drug gentamicin. *J. Struct. Chem*., **2017**, *58* (3), 462-470, DOI: 10.1134/S0022476617030064.

[43] Fehir, J.; Richard, J; McCusker, J. K., Differential polarization of spin and charge density in substituted phenoxy radicals. *J. Phys. Chem. A*, **2009**, *113* (32), 9249-9260, DOI: 10.1021/jp905314h.

[44] Wheelhouse, R. T., *et al*., Cationic porphyrins as telomerase inhibitors: the interaction of tetra-(N-methyl-4-pyridyl) porphine with quadruplex DNA. *JACS*, **1998**, *120* (13), 3261-3262, DOI: 10.1021/ja973792e.

[45] Wei, C.; Wang, J.; Zhang, M., Spectroscopic study on the binding of porphyrins to (G4T4G4) 4 parallel G-

quadruplex. *Biophy. Chem*., **2010**, *148* (1-3), 51-55, DOI: 10.1016/j.bpc.2010.02.009.

[46] Parkinson, G. N.; Ghosh, R.; Neidle, S., Structural basis for binding of porphyrin to human telomeres. *Biochem.*, **2007**, *46* (9), 2390-2397, DOI: 10.1021/bi062244n.